Structure and Properties of Novel Asymmetric Biphenyl Type Polyimides. Homo- and Copolymers and Blends

Masatoshi Hasegawa,*,† Nobuyuki Sensui,† Yoichi Shindo,† and Rikio Yokota‡

Department of Chemistry, Faculty of Science, Toho University, 2-2-1 Miyama, Funabashi, Chiba 274-8510 Japan, and Institute of Space and Astronautical Science, 3-1-1 Yoshinodai, Sagamihara, Kanagawa 229-0022, Japan

Received June 1, 1998

ABSTRACT: Asymmetric biphenyl type polyimides (PI) were prepared by thermal imidization of polyamic acids (PAA) derived from 2,3,3′,4′-biphenyltetracarboxylic dianhydride (a-BPDA) and *p*-phenylenediamine (PDA) or 4,4′-oxydianiline (ODA). The dynamic mechanical properties of these PIs were compared with those of the isomeric PIs derived from symmetric 3,4,3′,4′-biphenyltetracarboxylic dianhydride (s-BPDA). a-BPDA/PDA polyimide has a considerably bent chain structure compared to semirigid s-BPDA/PDA. Nevertheless, the a-BPDA/PDA film annealed at 350 °C showed a higher T_g than the s-BPDA/PDA film prepared under the same conditions. When these PIs were annealed at 400 °C, a-BPDA/PDA exhibited an abrupt E' decrease at the T_g (=410 °C) as well as the counterpart annealed at 350 °C, whereas s-BPDA/PDA showed no distinct T_g in the E' curve. Similar annealing effects were also observed for the ODA systems. The unexpectedly higher T_g's of a-BPDA-based PIs could be explained in terms of the more restricted conformational change through the crank shaft-like motion. The difference between the extents of the E' decrease at the T_g for a- and s-BPDA-based PIs is attributed to the difference of the intensity of intermolecular interactions. The blends of s-BPDA/PDA with a-BPDA-based PI (80/20) and the corresponding copolyimide improved the insufficient thermal processability of homo s-BPDA/PDA without causing a decrease in T_g. The results revealed that, for semirigid s-BPDA/PDA, a-BPDA-based PIs are better matrix polymers than s-BPDA/ODA.

Introduction

Structure−property relationships in polyimide (PI) systems have been extensively investigated as a main subject for practical applications.[1−6] Here, "structure" means in general the chemical structure of the PI chains. Numeral systematic studies revealed that the chain structure (stiffness) is the most important factor influencing directly their physical properties. Recently, the local ordering, which depends strongly on the manufacturing conditions, was observed by means of various techniques, and the role of the ordered structures for the properties was discussed.[4−6] The most extensively reported results deal with the Kapton type polyimide, PMDA/ODA, derived from pyromellitic dianhydride (PMDA) and ODA. So far, we have focused Upilex type PIs, i.e., s-BPDA/PDA and s-BPDA/ODA, and reported the improved mechanical properties of the homopolymers[7,8] and their composites,[9,10] the spontaneous molecular orientation phenomenon induced by thermal imidization,[11,12] and local ordered structure formation.[13,14] However, there are few reports on asymmetric biphenyl type PIs, since this monomer is not commercially available.[15−17] The present paper describes the properties of the new type of PIs derived from a-BPDA and discusses the comparison with the corresponding s-BPDA-based PIs. We focus here on the dynamic mechanical properties of a-BPDA-based homopolyimides and, in addition, the copolyimides and the blends containing a small content of a-BPDA component.

* Corresponding author. E-mail mhasegaw@chem.sci.toho-u.ac.jp.
† Toho University.
‡ Institute of Space and Astronautical Science.

Experimental Section

PAAs and Model Compounds. Figure 1 shows the chemical structures of PIs and the model compounds and their symbols, which are represented as X/Y (X = dianhydride, Y = diamine components) for homo PIs, X_1:X_2/Y for copolyimides, and M(X/Z) (Z = monoamine component) for PI model compounds. PAAs were prepared by adding the equimolar amount of dianhydride powder into the *N*,*N*-dimethylacetamide (DMAc) solution of diamine with continuous stirring at room temperature for several hours. DMAc was dried with molecular sieves 4A and then vacuum-distilled before use. The monomers used are s-BPDA (Wako Pure Chemicals), a-BPDA, PDA (Tokyo Chemical Industry, recrystallized from ethyl acetate), and ODA (Tokyo Chemical Industry, recrystallized from toluene/DMF (10/1, v/v)). a-BPDA,[18] which is a byproduct of s-BPDA, was supplied from Ube Industries Co. s-BPDA (without purification) and a-BPDA recrystallized from toluene/acetic anhydride (24/1, v/v) were both vacuum-dried at 200 °C for 24 h before polymerization. The reduced viscosities of PAAs (0.5 wt % in DMAc at 25 °C) were 2.57 dL g^{-1} for a-BPDA/PDA, 3.32 dL g^{-1} for s-BPDA/PDA, 1.60 dL g^{-1} for a-BPDA/ODA, and 2.00 dL g^{-1} for s-BPDA/ODA.

For preparation of PI model compounds, BPDA and the stoichiometric amount of cyclohexylamine (CHA) or aniline (AN) were stirred in DMAc at room temperature for 1 h; subsequently, the solution was refluxed at the boiling point for 1 h and cooled to room temperature. The crude products obtained by filtration were recrystallized twice from dichloroacetic acid for M(s-BPDA/AN), from toluene for M(s-BPDA/CHA), from DMAc for M(a-BPDA/AN) and M(a-BPDA/CHA), and from benzene for M(PA/CHA).

Homo and Blend PI Films. The DMAc solutions of PAA (10 wt %) were doctor-bladed on a glass substrate and then dried at 60 °C for 2 h in an air convection oven. The PAA films were removed from the substrate and then put into a glass tube equipped with a thermocouple. The evacuated glass tube was inserted into a preheated tubular furnace to imidize at 200 °C for 3 h (dwell time) + T_{ann} °C (temperature of additional annealing) for 1 h without substrate and frame, unless

10.1021/ma9808629 CCC: $18.00
Published on Web 12/29/1998

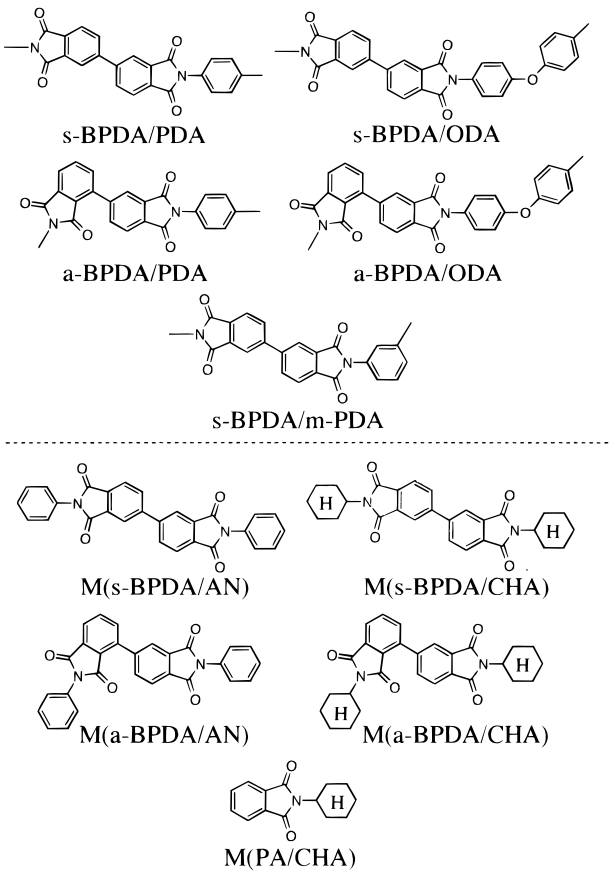

Figure 1. Chemical structures of polyimides and their model compounds used.

otherwise indicated. After annealing at T_{ann} °C for 1 h, the glass tube was cooled to room temperature within a few minutes. The temperature ramp for heating was not linear (sigmoid) for our furnace (the time required from room temperature to 200 °C: ca. 15 min). PAA binary blend films were prepared by casting at 60 °C immediately, after prompt mixing of two kinds of PAA solutions for 10 min at room temperature to suppress transamidation. The film thicknesses indicated in the text are all values of PI films.

Measurements. The coefficients of thermal expansion (CTE) of PI specimens (10 mm long, 5 mm wide, 10−20 μm thick) were measured as the average within 100−250 °C for the in-plane direction on a thermomechanical analyzer (Mac Science TMA-4010) with a load (0.5 g per thickness of 1 μm) in a nitrogen flow. The elongation of PAA films during a heating process (TMA curve) was recorded as a function of load.

The viscoelastic properties were measured using the same apparatus with a heating rate of 5 °C min^{-1} and a load frequency (sinusoidal) of 0.1 Hz in N_2. In this apparatus, the measurements are automatically interrupted when the film elongation exceeded 3000 μm. For the CTE and the dynamic mechanical measurements, the PI films cured on a substrate were annealed additionally at T_g−5 °C for 1 h in a free-standing state to remove the residual stress in the films.

Thermogravimetric analysis (TGA) (Mac Science TG-DTA 2000) for fully cured PI films and PAA cast films was conducted to estimate the chemical heat resistance and the amount of residual solvent in the PAA films with a heating rate of 10 °C min^{-1} in a N_2 flow.

Differential scanning calorimetry (DSC) was carried out using Mac Science DSC-3100 with 7 °C min^{-1} for PAA films and with 2 °C min^{-1} for the model compounds. A sealed aluminum pan was used for the model compounds to avoid sublimation of them during the heating process. The second runs of the DSC and TGA thermograms were taken after preheating to 100 °C to remove the adsorbed water.

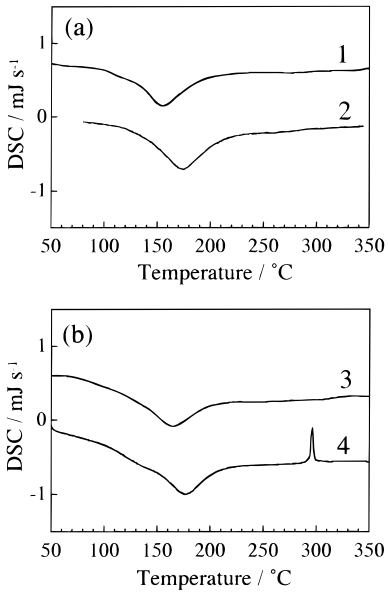

Figure 2. DSC thermograms for as-cast PAA films. (a) PDA systems: a-BPDA/PDA (1) and s-BPDA/PDA (2). (b) ODA systems: a-BPDA/ODA (3) and s-BPDA/ODA (4).

The densities of PI films prepared under various cure conditions were measured at 25 °C using a density gradient column (xylene−CCl_4 system).

Ultraviolet−visible absorption spectra of the model compounds in dichloromethane were recorded on Jasco V-520 spectrophotometer.

The relative amounts of the terminal anhydride groups in the thin PI films (3−4 μm thick) cast on a silicon wafer, formed during the stepwise heating process, were conventionally monitored by the absorbance ratio of the 1850 cm^{-1} (ν(C═O) in anhydride group) to 1515 cm^{-1} (internal standard: ν aromatics in the PDA moiety) bands.

Reflection mode WAXD measurements for PI films were conducted at room temperature on a Rigaku XRD-RAD2C (Cu Kα, 20 mA, 40 kV) with a sampling step of 0.1° and a scan rate of 5° min^{-1}.

Results and Discussion

Film Toughness Affected by Thermal Histories. a-BPDA/PDA as-cast PAA film was tough; namely, it did not break by folding up and slight stretching by hand. Nevertheless, thermal imidization of the PAA film in a free-standing state under our standard cure conditions (stepwise heating: 150 + 200 + 250 °C for 1 h each step) gave a very brittle PI film, whereas for s-BPDA/PDA good PI films were obtained under the same cure conditions. It was difficult to prepare thick a-BPDA/PDA films (>20 μm) through thermal imidization on a substrate or in a frame because of film cracking. Additionally, one-step (rapid) cure of the thick a-BPDA/PDA films above 300 °C provided films containing fine bubbles. We then searched the cure conditions required for preparing good a-BPDA/PDA PI films.

Figure 2a shows the DSC thermograms of the as-cast PAA films for the PDA system, a- and s-BPDA/PDA. The a-BPDA/PDA film showed an endothermic peak due to imidization at a lower temperature (154 °C) than the s-BPDA/PDA film (171 °C). A similar tendency was observed in the ODA system as shown in Figure 2b. These results correspond to the TGA curves (not shown) of these PAAs in which the weight loss due to imidization for a-BPDA/PDA started at a lower temperature than for s-BPDA/PDA. The higher imidization rate of a-BPDA/PDA is probably due to the higher local mobil-

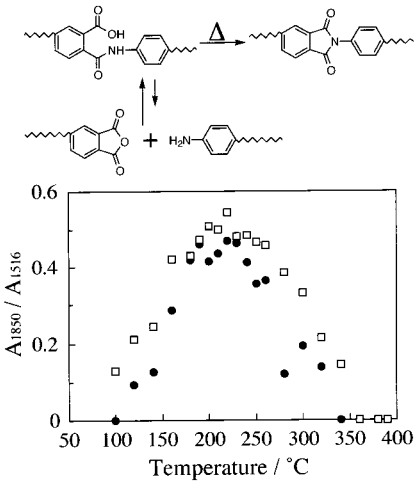

Figure 3. Relative amount of terminal anhydride group as a function of cure temperature in the stepwise heating process for PAA films: (□) a-BPDA/PDA and (●) s-BPDA/PDA.

ity at the reactive sites, since both PAA films retain almost the same amount of residual DMAc (20 wt %) as a plasticizer.

During thermal imidization, a reverse reaction of acylation (depolymerization) occurs partially to form the amino and anhydride terminal groups (Figure 3) and leads to a tentative molecular weight decrease, although the terminal groups recombine by additional annealing at higher temperatures. In general, the film brittleness is related to the initial molecular weight of PAAs and the extent of the reverse reaction during cure. Figure 3 also illustrates the relative amount of anhydride group as a function of cure temperature in the stepwise heating process. For a-BPDA/PDA, the anhydride group was formed in a wider temperature range than that for s-BPDA/PDA. However, annealing at $T_{ann} \geq 350$ °C promoted recombination reaction for both systems. This result corresponds to the fact that the a-BPDA/PDA brittle film cured at 250 °C in free-standing state became tough after additional annealing at $T_{ann} \geq 350$ °C.

Figure 4 displays the TMA curves of the as-cast PAA films of a- and s-BPDA/PDA as a function of load. Generally, unstretched PAA films show considerable elongation at 170−180 °C in the TMA curves, corresponding to the apparent T_g's of the partially imidized PAAs in the heating process. The s-BPDA/PDA film exhibited slight elongation at 180−190 °C after gradual shrinkage due to imidization in the range 100−170 °C (Figure 4b). On the other hand, the a-BPDA/PDA film did not elongate at the apparent T_g but shrank successively. The results indicate that cracking of the a-BPDA/PDA thick films cured on a substrate or in a frame is attributed to the combination of the higher extent of molecular weight decrease and the film shrinkage, which acts like stretching for the films fixed by substrate or frame.

On the other hand, the a-BPDA/ODA film did not become brittle even upon the cure at 250 °C, corresponding to the suppressed anhydride formation; the 1850/1515 absorption ratio was much lower (=0.035) at the maximum (not shown).

From now on, all the PI films were finally annealed at $T_{ann} \geq 350$ °C after precuring at 200 °C for 3 h.

Figure 5 shows the TGA curves of the fully cured a-BPDA-based PI and s-BPDA-based PI films. The

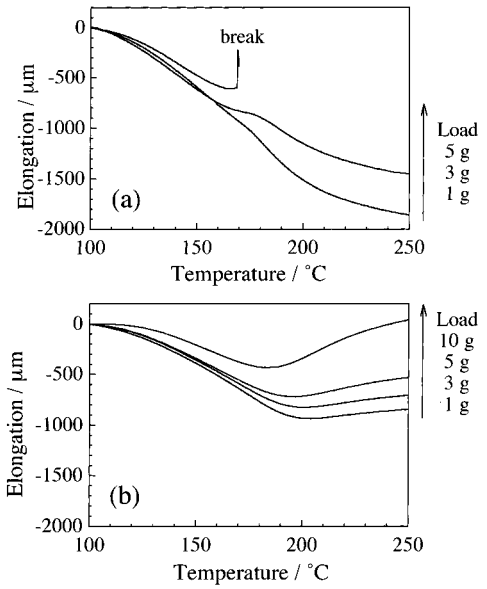

Figure 4. TMA curves of the PAA films (20 μm thick) of (a) a-BPDA/PDA and (b) s-BPDA/PDA as a function of load.

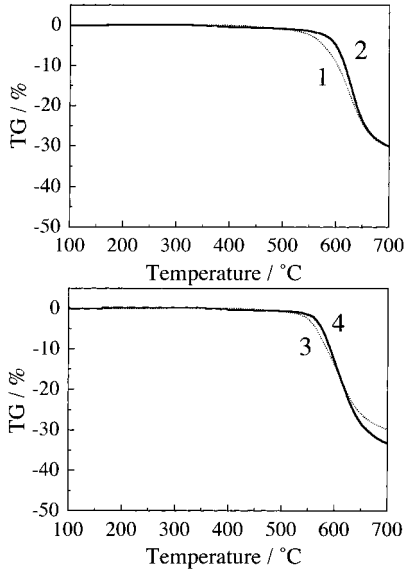

Figure 5. Weight loss curves of PI films with a heating rate of 10 °C min^{-1} in a nitrogen flow: (1) a-BPDA/PDA, (2) s-BPDA/PDA cured at 200 °C for 3 h + 400 °C for 1 h, (3) a-BPDA/ODA, (4) s-BPDA/ODA cured at 200 °C for 3 h + 350 °C for 1 h.

former has thermal stability a little lower than those of the latter for both PDA and ODA systems. However, considerably high thermal stability was confirmed for both a-BPDA-based PIs. From the results, we determined the upper limit of annealing temperature to be 400 °C for a-BPDA-based PIs.

Dynamic Mechanical Properties of a- and s-BPDA-Based PI Films. Figure 6 displays the dynamic storage modulus (E') and loss energy (E'') as a function of temperature for the s-BPDA/PDA and a-BPDA/PDA films cured at 200 °C/3 h + 350 °C/1 h in a free-standing state. Regarding the peak temperature in the E'' curves as the T_g, semirigid s-BPDA/PDA exhibited a T_g at 355 °C; on the other hand, a-BPDA/PDA with a bent chain structure showed an unexpectedly higher T_g at 385 °C. For s-BPDA/PDA, E' decreased at the T_g more gradually than that for a-BPDA/PDA. This is often observed in highly cross-linked or highly crystallized polymers.[19] It

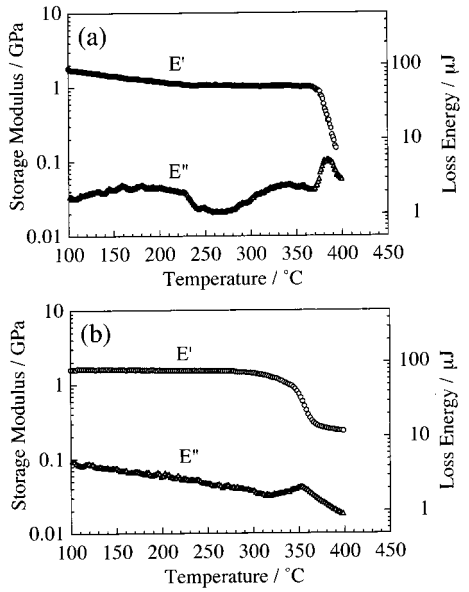

Figure 6. Dynamic storage modulus (E') and loss energy (E'') as a function of temperature for PI films cured at 200 °C for 3 h + 350 °C for 1 h: (a) a-BPDA/PDA (17 μm thick) and (b) s-BPDA/PDA (14 μm thick).

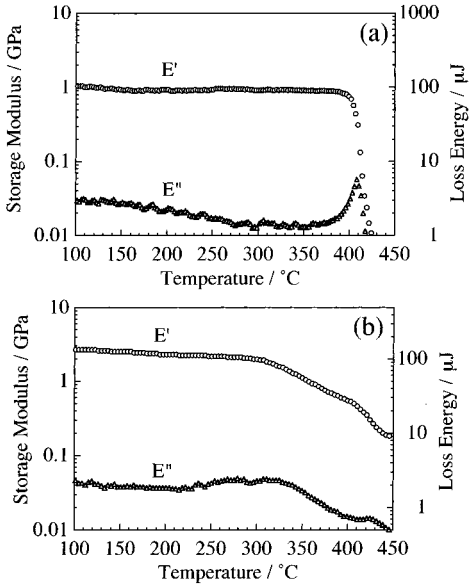

Figure 7. E' and E'' curves for PI films cured at 200 °C for 3 h + 400 °C for 1 h: (a) a-BPDA/PDA (13 μm thick) and (b) s-BPDA/PDA (12 μm thick).

is understandable that the rodlike segments of s-BPDA/PDA induces strong interchain interactions and consequently forms crystallike order.[14] However, the higher T_g of a-BPDA/PDA is not readily explained from a general consideration that the introduction of a kink point, e.g., −O−, −S−, −CH_2−, −SO_2−, −CO−, into the repeating unit of a rigid PI main chain should decrease the T_g's significantly.[20] We discuss this inconsistency later.

Figure 7 illustrates the effect of annealing at a higher temperature on the E' and E'' curves. a-BPDA/PDA annealed at 400 °C showed an E' curve similar to that annealed at 350 °C except for the T_g increase of ca. 20 °C. On the other hand, for s-BPDA/PDA, the annealing at 400 °C led to a drastic change in the E' curve; no distinct glass transition was observed. Some probable factors for disappearance of the T_g are a decrease in the

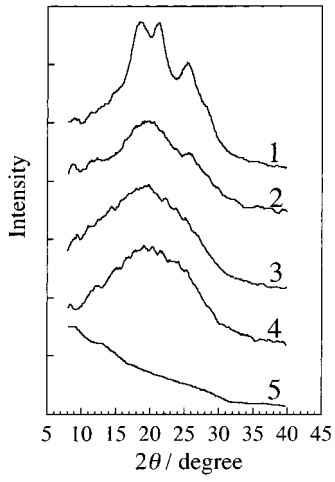

Figure 8. Reflection mode WAXD patterns of s-BPDA/PDA (1−4) and a-BPDA/PDA (5) films cured at 200 °C for 3 h + T_{ann} °C for 1 h: (1) T_{ann} = 400, (2) 350, (3) 300, (4) 250, and (5) 400 °C.

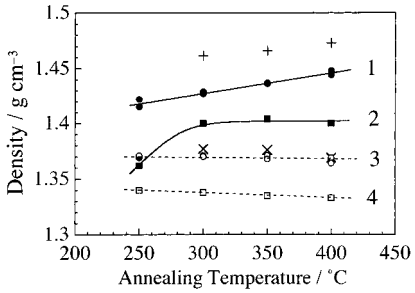

Figure 9. Changes in film density with an increase in annealing temperature (T_{ann}): (1) s-BPDA/PDA, (2) s-BPDA/ODA, (3) a-BPDA/PDA, and (4) a-BPDA/ODA. PAA films were cured at 200 °C for 3 h before annealing at T_{ann} for 1 h. For comparison, the densities of the one-step cured PI films were also plotted: (+) s-BPDA/PDA and (×) a-BPDA/PDA.

amorphous fraction (increase in crystallinity, X_c)[21] and intensification of the interchain interactions in the amorphous region such as the formation of ordered structure[14] and charge-transfer (CT) complex[13] which behave like physical cross-links. Figure 8 displays the reflection mode WAXD patterns of a- and s-BPDA/PDA films prepared under the same thermal conditions (200 + T_{ann} °C; T_{ann} = 250, 300, 350, and 400 °C). For s-BPDA/PDA, the sign of crystallization in the patterns became prominent with the increase in T_{ann} (curves 1−4), suggesting a decrease in the amorphous fraction. Such a prominent annealing effect is also known in the PMDA/ODA system (PMDA = pyromellitic dianhydride).[22] On the other hand, the a-BPDA/PDA film cured at 200 °C/3 h + 400 °C/1 h provided a typical amorphous pattern (curve 5), which did not depend on T_{ann} (not shown).

The film density, which represents the degree of molecular packing, of s-BPDA/PDA (curve 1) increased markedly with increasing T_{ann}, whereas that of a-BPDA/PDA (curve 3) decreased only slightly as shown in Figure 9. For s-BPDA/PDA, the one-step cure of the PAA films at T > 300 °C, which provides more intensive molecular motion than the two-step cure (200 °C for 3 h + T_{ann} °C for 1 h), led to the higher film densities (Figure 9). On the other hand, the one-step cure for a-BPDA/PDA was less effective. The results suggest that s-BPDA/PDA can take a higher degree of molecular packing and stronger intermolecular interactions by

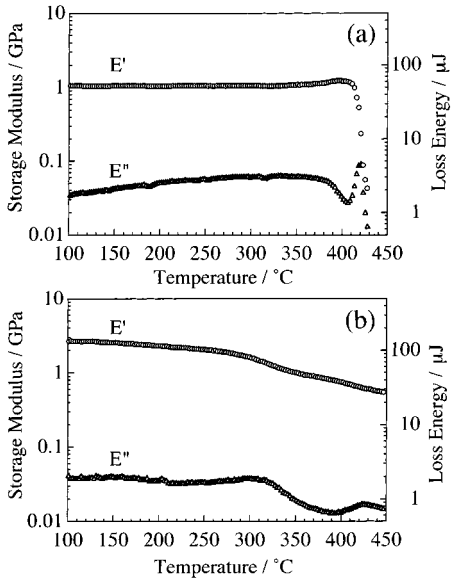

Figure 10. E' and E'' curves for PI films cured at 400 °C for 1 h (one-step): (a) a-BPDA/PDA (19 μm thick) and (b) s-BPDA/PDA (12 μm thick).

annealing, but a-BPDA/PDA cannot. The density results correspond well to the effect of the one-step cure on the E' curves for a- and s-BPDA/PDA (Figure 10). For s-BPDA/PDA, the one-step cure at 400 °C/1 h obviously made the E' reduction more indistinct than the two-step cure at 200 °C/3 h + 400 °C/1 h, but the E' curve of the one-step cured a-BPDA/PDA did not practically differ from that of the two-step cured sample. Thus, the effects of T_{ann} and cure history (one-step/two-step) on the E' curves for s- and a-BPDA/PDA are closely related to the morphological changes illustrated by the WAXD and density data.

Parts a and b of Figure 11 show a T_{ann} effect on the E' curves for the ODA systems, a- and s-BPDA/ODA, respectively. As in the PDA systems described above, the a-BPDA-derived PI film showed a more distinct glass transition and a higher T_g than s-BPDA/ODA. No practical T_{ann} effect on the extent of softening at the T_g's was observed for the a-BPDA/ODA system except for a slight T_g increase, corresponding to the fact that even the a-BPDA/ODA film prepared at T_{ann} = 350 °C/1 h is amorphous from the WAXD pattern (Figure 12, curve 4), which did not depend on T_{ann} (not shown). On the other hand, the E' curve of s-BPDA/ODA varied drastically with increasing T_{ann}; as the thermal conditions become more severe, going from (a) to (c), the extent of softening at the T_g reduced without appreciable T_g shift.[23]

Some probable factors for the significant change in the E' curve of s-BPDA/ODA are a decrease in the amorphous fraction due to crystallization[24] or crystallike local ordering[25] and intensification of interchain interactions in the amorphous region such as CT complex formation.[13] A sign of crystallization was observed with increasing T_{ann} in the WAXD patterns in Figure 12 (curves 1−3), although the pattern change was less prominent compared to the s-BPDA/PDA system (Figure 8). We also observed, when the completely amorphous s-BPDA/ODA film cured at 250 °C was additionally annealed at $T_{ann} \geq$ 300 °C, the crystal-field splittings in some structure-sensitive infrared bands in the range 1100−400 cm^{-1}, and these bands become well-resolved with increasing T_{ann}. The critical T_{ann} (=300 °C) corresponds to a precrystallization exothothermic peak at 295 °C in the DSC heating scans for the amorphous s-BPDA/ODA film cured at 250 °C (Figure 2b).[24] It should be noted that in principle the FTIR spectra reflect sensitively the much shorter range ordered structures than WAXD. The combined results of WAXD and FTIR suggest that the crystal size for s-BPDA/ODA is still very small even in the PI film annealed at 350 °C. We conclude that, in comparison of the s-BPDA/ODA films annealed at T_{ann} = 300 and 350 °C, the decreased plasticity at the T_g for the 350 °C sample is due to either a decrease in the amorphous fraction or an increase in

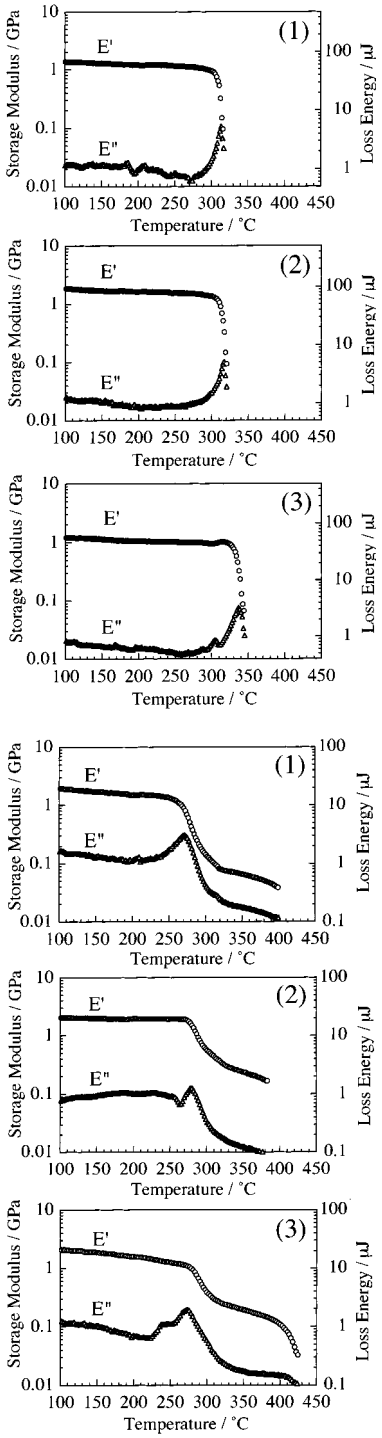

Figure 11. E' and E'' curves for (a, upper) a-BPDA/ODA (10−12 μm thick) and (b, lower) s-BPDA/ODA (10−14 μm thick) films: (1) cured at 200 °C/3 h + 300 °C/1 h, (2) 200 °C/3 h + 350 °C/1 h, and (3) 400 °C/1 h (one-step cure on substrate).

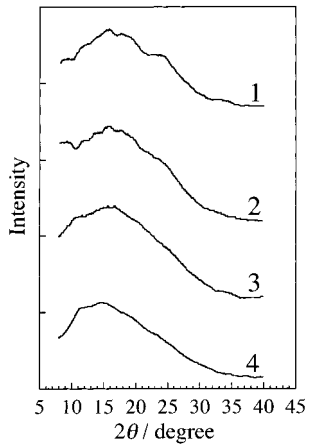

Figure 12. Reflection mode WAXD patterns of s-BPDA/ODA (1−3) and a-BPDA/ODA (4) films cured at 200 °C for 3 h + T_{ann} °C for 1 h: (1) T_{ann} = 350, (2) 300, (3) 250, and (4) 350 °C.

the crystal size (but still very small) without significant change in X_c.

As shown in Figure 9, the density of the s-BPDA/ODA film increased abruptly at T_{ann} = 300 °C, corresponding to crystallization induced by annealing at $T_{ann} \geq 300$ °C. However, the density of the film leveled off above 300 °C in contrast to the T_{ann} effects on the WAXD patterns, FTIR spectra, and E' curves. This density result may suggest that the 350 and 300 °C samples do not differ significantly in the X_c from each other but do in the crystal size. On the other hand, no T_{ann} effect on the film density was observed for a-BPDA/ODA. The film densities of a-BPDA/ODA were much lower than those of s-BPDA/ODA, indicating a lower degree of molecular packing (weaker intermolecular interactions) in a-BPDA/ODA.

Factors Influencing the T_g's of a-BPDA-Based PIs. Next, we studied the unexpectedly higher T_g's of a-BPDA-based PIs with the bent chain structure. The T_g's of linear polymers are in general dominated by intramolecular interactions (the chain linearity, rotational barrier for conformational change) and intermolecular interactions (hydrogen bonding, dipole−dipole and CT interactions, etc.). For a-BPDA-based PIs, the latter factors do not significantly contribute to the increased T_g's, since the steeply bent chain structure makes the molecular packing looser and consequently prevents strong intermolecular interactions. The higher T_g's of a-BPDA-based PIs seem to be contradictory to many results for the structure−T_g relationship in PI systems. Bessonov et al.[20] demonstrated that the introduction of the bent points such as ether linkage into PI chains, especially into the diimide portions, reduces markedly the T_g. They classified a variety of aromatic PIs into four groups based on the position and number of the bent points in the structure. They treated these bent points as a hinge and took into account the dipole−dipole interchain interactions between imide carbonyl groups. For illustrating the relation between the chain linearity and T_g, there is a good example, i.e., comparison of PIs derived from three isomers, 3,4,3′,4′-, 2,3,3′,4′-, and 2,3,2′,3′-oxydiphthalic anhydride (ODPA) with PDA. Indeed, a decrease in the chain linearity (3,4,3′,4′-ODPA > 2,3,3′,4′-ODPA > 2,3,2′,3′-ODPA) caused a reduction in the T_g (326 °C for 3,4,3′,4′-ODPA, 313 °C for 2,3,3′,4′-ODPA, and 294 °C for 2,3,2′,3′-ODPA where the T_g's were measured by DSC).[26,27] However, in fact, this criterion conflicts with our results of the T_g's for a- and s-BPDA-based PIs. This is probably the reason why the rotational flexibility at the ether linkage in the ODPA unit is much higher than that at the biphenyl linkage in the BPDA moiety.[28]

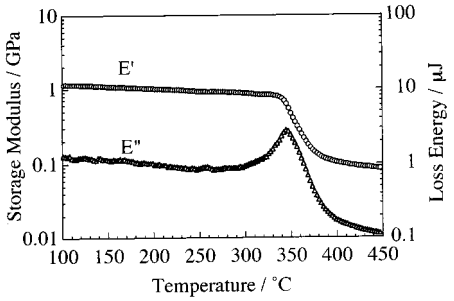

Figure 13. E' and E'' curves for s-BPDA/m-PDA (15 μm thick) film cured at 200 °C for 3 h + 400 °C for 1 h.

Table 1. T_m, ΔH_m, and ΔS_m Obtained by DSC Measurements (2 °C min^{-1}) for PI Model Compounds, M(a-BPDA/AN) and M(s-BPDA/AN)

model compds	T_m/°C	ΔH_m/kJ mol^{-1}	ΔS_m/J mol^{-1} K^{-1}
M(a-BPDA/AN)	307	49.1	84.6
M(s-BPDA/AN)	390	44.1	66.5

We considered the meta-phenylene group as another type of the bent point. Figure 13 displays the E' and E'' curves of s-BPDA/m-PDA. This PI showed a T_g at 345 °C lower than that of s-BPDA/PDA (T_g = 360−370 °C[29]), according to the general consideration for the structure−T_g relationship. What is the reason for the higher T_g of a-BPDA/PDA (T_g = 405 °C) than that of s-BPDA/PDA? A possible explanation is that the internal rotation at the biphenyl bonds in the a-BPDA moiety is more restricted. To confirm this assumption thermodynamically, we first attempted to consider it from the entropy changes for melting, ΔS_m of PI model compounds.[30]

(a) Model Compound Approach. An empirical relation, $T_m \approx 1.3T_g$ (in kelvin),[20] is known for flexible PI systems containing the ether linkages. According to this relation, it is expected from the comparison of the T_g's of a-BPDA/PDA and s-BPDA/PDA that the former has a higher T_m than the latter. The T_m measurements by DSC can also provide the enthalpy change, ΔH_m and ΔS_m ($=\Delta H_m/T_m$). However, it is impossible to obtain experimentally these thermodynamic parameters for amorphous polymers without T_m (e.g., a-BPDA-based PIs) and polymers with T_m's higher than their thermal decomposition temperatures (e.g., s-BPDA/PDA).

An alternative approach is to use low molecular weight model compounds. The T_m's of the PMDA-type model compounds have a tendency to increase with increasing T_g of the corresponding PIs.[31] This empirical relation leads to an expectation that M(a-BPDA/AN) has a higher T_m than M(s-BPDA/AN). Additionally, we predicted first that M(a-BPDA/AN) shows a lower ΔS_m and lower ΔH_m from the assumptions mentioned previously: (1) the rotational motion at the biphenyl linkage in the a-BPDA unit is more strongly suppressed than that in the s-BPDA unit, and (2) intermolecular interactions are much weaker for a-BPDA systems. However, as listed in Table 1, the values of T_m, ΔH_m, and ΔS_m for two model compounds were quite contrary to our first expectation; M(a-BPDA/AN) provided a lower T_m, a higher ΔS_m, and a higher ΔH_m than M(s-BPDA/AN). Thus, we could not confirm the more restricted conformational motion at the a-BPDA unit from the model compound approach. A possible explanation for the

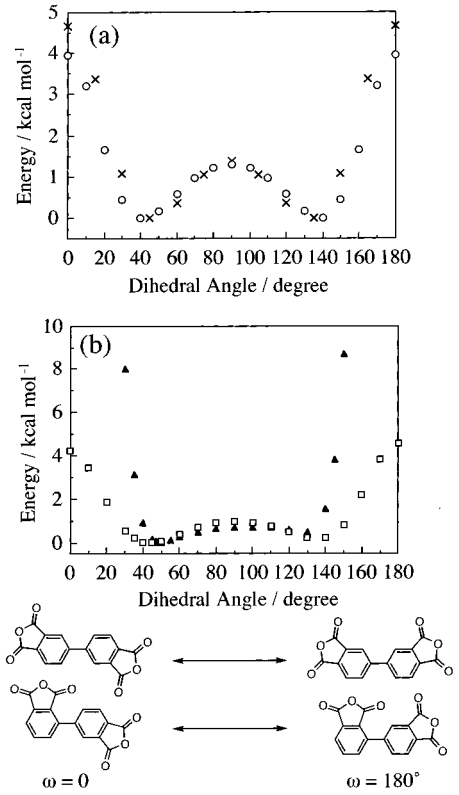

Figure 14. Potential energies as a function of the dihedral angle for biphenyl compounds, obtained with the semiempirical MO calculation (MOPAC93, AM1): (a) (○) biphenyl in the present work, (×) biphenyl in ref 32 (GAUSSIAN94, 6-31G); (b) (▲) a-BPDA, (□) s-BPDA.

unexpectedly lower ΔS_m for M(s-BPDA/AN) is that some intermolecular interactions may still remain even at the molten state, leading to a decreased diffusional mobility in the molten state M(s-BPDA/AN) molecules. This assumption does not conflict with the fact that the ΔH_m of M(s-BPDA/AN) was unexpectedly lower than that of M(a-BPDA/AN) and additionally reminds us the reason why the s-BPDA/PDA PI film annealed at 400 °C has no distinct glass transition. The fact that the model compound approach failed to explain the higher T_g's of a-BPDA-based PIs may suggest that some modes of longer range conformational change should be considered.

(b) Conformational Changes of a- and s-BPDA/PDA. Next, we examined the rotational flexibility at the a- and s-BPDA units. Figure 14b indicates the potential energies as a function of dihedral angle (ω) at the biphenyl bonds for a- and s-BPDA in the gas phase, as obtained by the semiempirical molecular orbital calculation (MOPAC93, potential function: AM1). For comparison, the rotational energies of biphenyl were also calculated in the same way (Figure 14a), providing an energy surface very similar to that calculated by others using the ab initio method (GAUSSIAN94, basis set: 6-31G).[32] The results suggest that s-BPDA provides a very similar potential surface to that of biphenyl. On the other hand, a-BPDA has a rotational barrier much higher at $\omega = 0°$ than s-BPDA owing to the expected steric hindrance between the orthohydrogen atoms and the 2-carbonyl group of a-BPDA. The lower rotational barrier at $\omega = 0°$ for s-BPDA (~4 kcal mol^{-1}) does not always mean that the internal rotation is allowed beyond the barriers at the coplanar state. Even in the rubbery state at $T > T_g$, the potential barriers for both

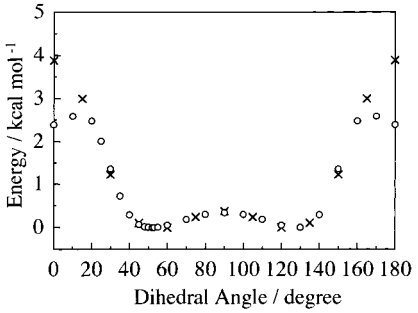

Figure 15. Potential energy of *N*-phenylphthalimide as a function of the dihedral angle, obtained with the semiempirical MO calculation (MOPAC93, PM3): (○) the present work, (×) ref 32 (GAUSSIAN-94, 6-31G**).

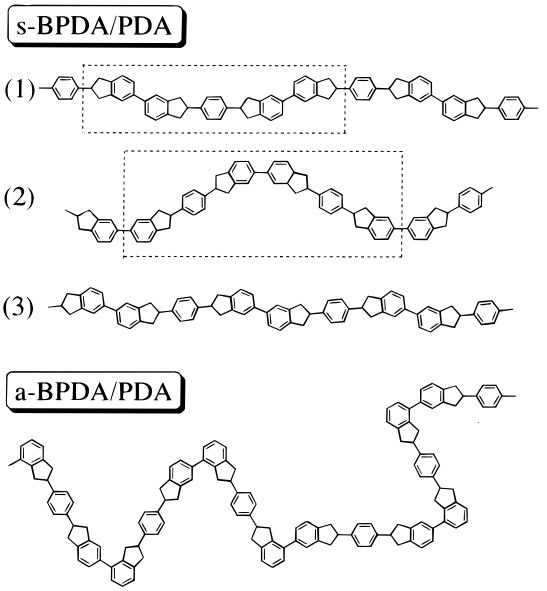

Figure 16. Schematic diagram for the conformational changes through the crank shaft motion: (a) s-BPDA/PDA and (b) a-BPDAPDA. The structures are simplified.

the s- and a-BPDA units are probably high enough to inhibit the free rotation beyond the coplanar state. Accordingly, we consider that there is no significant difference in the rotational flexibility between a- and s-BPDA; only local rotational motions within $\omega = 50-130°$ for a-BPDA and $\omega = 40-140°$ for s-BPDA are allowed beyond the very low barriers at $\omega = 90°$.

On the other hand, a-BPDA/PDA and s-BPDA/PDA commonly have the N−1,4-phenylene−N fragment. Accordingly, there is no difference in the rotational flexibility at the N−phenyl linkages in both PIs. *N*-phenylphthalimide provided a potential energy surface similar to that of s-BPDA as shown in Figure 15. This suggests that the rotational motion around the N−phenyl linkage probably occurs within $\omega = 50-130°$. Thus, the higher T_g of a-BPDA/PDA could not be explained in terms of the more suppressed local rotational flexibilities at the biphenyl linkage.

Alternatively, it is necessary to consider the longer range conformational change mode. Figure 16 schematically depicts the profiles of predicted cooperative conformational changes for s-BPDA/PDA. Semirigid s-BPDA/PDA is known to take the extended chain form as evidenced by the sharp (004) peak in the transmission mode WAXD patterns.[21] For simplicity, we present here three types of the extended chain conformation of the s-BPDA/PDA chains with the coplanar structure. For

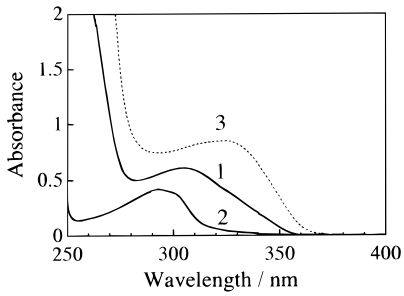

Figure 17. Ultraviolet−visible absorption spectra of the PI model compounds in dichloromethane (1.00×10^{-4} M): (1) M(a-BPDA/CHA), (2) M(PA/CHA) (×2), and (3) M(s-BPDA/CHA).

types (1) and (2), cooperative rotational motions of the portions surrounded by broken line are possible around the N−phenyl ($\omega = 50-130°$) and the biphenyl ($\omega = 40-140°$) bonds through a "crank shaft"-like motion. The most extended chain conformation (3) allows no cooperative motions. On the other hand, for a-BPDA/PDA with bent chain structure, one can readily suppose that no cooperative conformational change is possible since it can take no extended forms. For a-BPDA/PDA, even if such a cooperative rotational motion is possible, a sweep volume much larger than that for s-BPDA/PDA should be required for the crank shaft motion. Thus, the higher T_g of a-BPDA-based PIs could be explained in terms of the difficulty of the cooperative conformational changes.

Figure 14b also indicates that the most stable dihedral angle at the a-BPDA unit ($\omega = 49°$) is higher than that at the s-BPDA unit ($\omega = 40°$). These values were calculated for the gaseous phases. However, taking into account the fact that biphenyl can often take the coplanar state in the crystalline phase,[33] the biphenyl dihedral angles in the solid (film) state, especially for s-BPDA/PDA, probably differ from those calculated for gaseous phase owing to the presence of interchain interactions in the film. This also suggests that the biphenyl conformation in s-BPDA/PDA may depend on cure conditions and the degree of chain orientation, although there is no available method to monitor the biphenyl conformation in the PI film state. On the other hand, for a-BPDA/PDA, which cannot take the coplanar state owing to the orthohydrogen/2-carbonyl steric hindrance, one expects that the biphenyl conformation does not depend on cure conditions. This corresponds to the morphology independent of cure conditions as described previously.

Ultraviolet−visible (UV−vis) absorption spectra of biphenyl derivatives provide qualitative information on the biphenyl conformation in solution; when $\omega \approx 90°$, the absorption spectrum becomes similar to the 2-fold spectrum of the corresponding monomeric unit (phenyl derivatives) owing to the sterically inhibited conjugation, but a peak red shift and enhancement of the band intensity become prominent as it approaches coplanar structure.[34,35] According to this criterion, we compared M(a-BPDA/CHA) with M(PA/CHA) as its monomeric derivatives, since the corresponding aniline (AN)-derived model compounds do not show a distinct peak of the (π,π*) band.[16,36] Figure 17 shows the absorption spectra of these model compounds in solution, together with M(s-BPDA/CHA). M(a-BPDA/CHA) exhibited a stronger and red-shifted spectrum compared to the 2-fold of the M(PA/CHA) spectrum, suggesting qualitatively that a-BPDA has a ω lower than 90°. Unfortunately, we could not compare the spectra of M(a-BPDA/CHA) and M(s-BPDA/CHA) to discuss their ω's, since these compounds have different conjugation due to different positions of the carbonyl substituents.

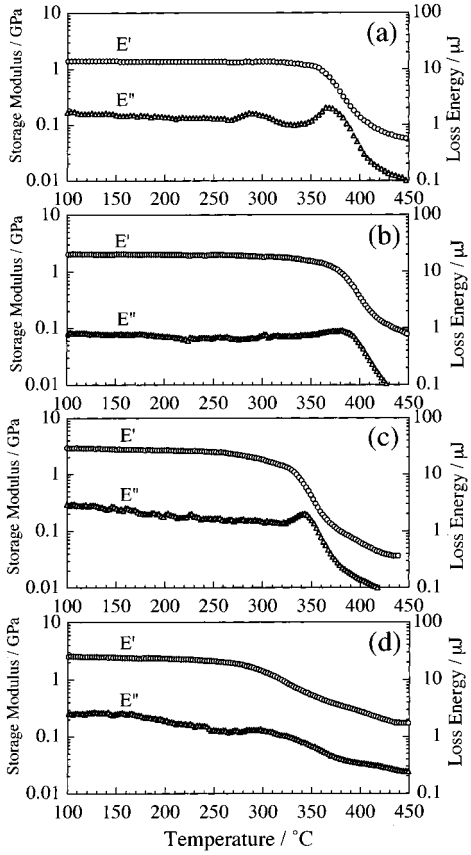

Figure 18. E' and E'' curves for s-BPDA/PDA-based copolymer and blends with the composition of a-BPDA = 20 mol %, cured at 200 °C for 3 h + 400 °C for 1 h: (a) s-BPDA:a-BPDA/PDA copolyimide (13 μm thick), (b) s-BPDA/PDA/a-BPDA/PDA blend (8 μm thick), (c) s-BPDA/PDA/a-BPDA/ODA blend (12 μm thick), and (d) s-BPDA/PDA/s-BPDA/ODA blend (9 μm thick).

The s-BPDA/t-CHDA (t-CHDA = *trans*-1,4-cyclohexanediamine) and a-BPDA/t-CHDA thin films cured at 250 °C/1 h on a quartz plate showed UV−vis absorption spectra similar to those of the respective model compounds. We attempted to examine an annealing effect on the spectral position and intensity (change in the biphenyl conformation) for both PIs, but it was disturbed by coloration due to thermal decomposition caused by an increase in T_{ann}.

Properties of Blends and Copolymers Containing a-BPDA. s-BPDA/PDA is widely known to show some excellent properties such as high thermal stability, low CTE, and high modulus, while it has no thermal plasticity. Improvement of the thermal plasticity is required for compression molding of s-BPDA/PDA. According to the above-described results that a-BPDA-based PIs show higher thermal plasticity at $T > T_g$, it is most likely expected that the blending with a-BPDA-based PIs or copolymerization with a-BPDA improves the insufficient thermal processability of s-BPDA/PDA homopolymer without a decrease in the T_g.

We examined the dynamic mechanical properties and CTE of the blends and the copolymers over the wide a-BPDA composition range (10−90 mol %). Figure 18a−c exhibits some typical E' and E'' curves of the

Table 2. CTE of Homopolyimides, Copolyimide, and Blends Shown in Figure 18

type	symbol	thickness/ μm	sub-strate	CTE/ ppm
homo-polymer	s-BPDA/PDA	7	on	9.1
	s-BPDA/PDA	11	off	11.8
	a-BPDA/PDA	5	on	58.0
	s-BPDA/PDA	13	off	59.1
	s-BPDA/ODA	15	on	56.0
	a-BPDA/ODA	15	off	62.0
copolymer	s-BPDA(80):a-BPDA(20)/PDA	9	on	17.4
blend	s-BPDA/PDA(80)/a-BPDA/PDA(20)			
	s-BPDA/PDA(80)/a-BPDA/ODA(20)			
	s-BPDA/PDA(80)/s-BPDA/ODA(20)			

copolymers and the blends with a-BPDA = 20%. s-BPDA:a-BPDA/PDA copolyimide showed a more prominent softening at the T_g, namely, higher thermal plasticity than s-BPDA/PDA homopolymer, but the copolyimide with a-BPDA = 10% did not. As the a-BPDA composition is increased (>30 mol %), the thermal plasticity (the extent of E' decrease at the T_g) of the copolyimide films became higher. Since the values of CTE for a-BPDA-based homo PIs are very high, a certain degree of CTE increase by introducing the a-BPDA unit (20%) is inevitable as listed in Table 2. Similar dependence of the E' curves on the a-BPDA content was also observed in two s-BPDA/PDA-based blend systems containing a-BPDA/PDA or a-BPDA/ODA. As shown in Figure 18a,b, the E' curve for the copolyimide with a-BPDA = 20% is similar to that for the corresponding blend, except for that the T_g of the blend is about 5 °C higher than that of the copolymer. The addition of a-BPDA/ODA as a flexible component also provides thermal plasticity at $T > T_g$, although the T_g of the blend is lower than that of the a-BPDA/PDA-containing blend. Thus, a-BPDA was applied successfully for improvement of the thermal processability of s-BPDA/PDA.

The improved plasticity results from the good miscibility of these blends, as demonstrated from the fact that the single T_g for both blends changed depending on the blend composition. However, in contrast to the a-BPDA-containing blends, the blend containing s-BPDA/ODA as a flexible component showed a very broad E' decrease. This most likely results from crystallization of the s-BPDA/ODA component by annealing at 400 °C as described previously (see Figures 11 and 12); in other words, this blend is in phase separation. These results reveal how the a-BPDA-based PIs are good matrix polymers which improve thermal processability.

Conclusions

Annealing at $T_{ann} > 350$ °C is required for obtaining highly tough a-BPDA/PDA films, relating to the recombination of the terminal groups formed during cure at $T < 300$ °C.

a-BPDA-based PIs provided higher T_g's than the corresponding s-BPDA-based PIs. The results could be explained in terms of the more restricted conformational changes in the a-BPDA-based PI chains.

s-BPDA/PDA showed a marked T_{ann} effect on the E' curves, but a-BPDA/PDA did not except for slight increase in the T_g with increasing T_{ann}. The indistinct glass transition of the s-BPDA/PDA film annealed at 400 °C is attributed to the decreased amorphous fraction. On the other hand, the abrupt E' decrease at the T_g for a-BPDA-based PIs is related to the fact that these PIs can take no ordered structure owing to the steeply bent chain structure.

The blend of s-BPDA/PDA and a-BPDA/PDA (80/20) gave a certain degree of thermal plasticity at $T > T_g$ and a higher T_g than that of s-BPDA/PDA homopolymer, as well as the corresponding copolyimide.

The blend of s-BPDA/PDA and a-BPDA/ODA (80/20) also exhibited thermal plasticity, whereas the blend of s-BPDA/PDA and s-BPDA/ODA (80/20) did not. This is attributed to crystallization of the s-BPDA/ODA component by annealing at 400 °C. These results revealed how a-BPDA-based PIs are good matrix polymers which provide good miscibility with s-BPDA/PDA and improved thermal processability.

Acknowledgment. We thank Dr. H. Yamaguchi of Ube Industries, Co., for receiving a-BPDA, Dr. Y. Tokita of Denki Kagaku Kogyo Co.Ltd. for his valuable comments for the MO calculations, and Dr. K. Katsuki for her experimental support for WAXD measurements.

References and Notes

(1) *Polyimides: Synthesis, Characterization, and Applications*; Mittal, K. L., Ed.; Plenum Press: New York, 1984.
(2) *Polyimides: Thermally Stable Polymers*; Bessonov, M. I., Koton, M. M., Kudryavtsev, V. V., Laius, L. A., Eds.; Consultants Bureau, A Division of Plenum Publishing Co.: New York, 1987.
(3) *Polyimides: Materials, Chemistry, and Characterization*; Feger, C., Khojasteh, M. M., MacGrath, J. M., Eds.; Elsevier: Amsterdam, 1989.
(4) *Polyamic Acids and Polyimides: Synthesis, Transformations, and Structure*; Bessonov, M. I., Zubkov, V. A., Eds.; CRC Press: Boca Raton, FL, 1993.
(5) *Polyimides: Trends in Materials and Applications*; Feger, C., Khojasteh, M. M., Molis, S. E., Eds.; Society of Plastic Engineers, Mid Hudson Section: New York, 1996.
(6) *Polyimides: Fundamentals and Applications*; Ghosh, M. K., Mittal, K. L., Eds.; Marcel Dekker: New York, 1996.
(7) Kochi, M.; Uruji, T.; Iizuka, T.; Mita, I.; Yokota, R. *J. Polym. Sci., Part C* **1987**, *25*, 441.
(8) Kochi, M.; Yonezawa, T.; Mita, I.; Yokota, R. In *Advances in Polyimide Science and Technology*; Feger, C., et al., Eds.; Technomic Publishing Co.: Lancaster, 1993; p 375.
(9) Yokota, R.; Horiuchi, R.; Kochi, M.; Soma, H.; Mita, I. *J. Polym. Sci., Part C* **1988**, *26*, 215.
(10) Yokota, R.; Horiuchi, R.; Kochi, M.; Takahashi, C.; Soma, H.; Mita, I. In *Polyimides: Materials, Chemistry, and Characterization*; Feger, C., Khojasteh, M. M., MacGrath, J. M., Eds.; Elsevier: Amsterdam, 1989; p 13.
(11) Hasegawa, M.; Matano, T.; Shindo, Y.; Sugimura, T. *Macromolecules* **1996**, *29*, 7897.
(12) Hasegawa, M.; Okuda, K.; Horimoto, M.; Shindo, Y.; Yokota, R.; Kochi, M. *Macromolecules* **1997**, *30*, 5745.
(13) Hasegawa, M.; Kochi, M.; Mita, I.; Yokota, R. *Eur. Polym. J.* **1989**, *25*, 349.
(14) Vladimirov, L.; Hasegawa, M.; Yokota, R. *Network Polym.* **1998**, *19*, 18.
(15) Inoue, H.; Okamoto, H.; Hiraoka, Y. *Radiat. Phys. Chem.* **1987**, *29*, 283.
(16) Hasegawa, M.; Sensui, N.; Shindo, Y.; Yokota, R. *J. Photopolym. Sci. Technol.* **1996**, *9*, 367.
(17) Yamaguchi, H. In *Recent Advances in Polyimides 1997* (*Proceedings of Japan Polyimide Conference '96*, Tokyo); Yokota, R., Hasegawa, M., Eds.; Raytech Co.: Tokyo, 1997; p 5.
(18) Iatatani, H.; Yoshimoto, H. *J. Org. Chem.* **1973**, *38*, 76.
(19) Nielsen, L. E. *Mechanical Properties of Polymers and Composites*; Marcel Dekker: New York, 1975.
(20) Bessonov, M. I.; Kuznetsov, N. P. In *Polyimides: Synthesis, Characterization and Applications*; Mittal, K. L., Ed.; Plenum Press: New York, 1984; p 385.
(21) Coburn, J. C.; Pottiger, M. T. In *Polyimides: Fundamentals and Applications*; Ghosh, M. K., Mittal, K. L., Eds.; Marcel Dekker: New York, 1996; p 207.
(22) Isoda, S.; Kochi, M.; Kambe, H. *J. Polym. Sci., Polym. Phys. Ed.* **1982**, *20*, 837.

(23) For the s-BPDA/ODA film cured at 250 °C, E' decrease at the T_g (=280 °C) occurs more drastically than that for the counterpart annealed at 300 °C (see Figure 11a). The s-BPDA/ODA film cured at 250 °C shows a distinct T_g at 280 °C in the DSC thermogram, which is consistent with that obtained by the dynamic mechanical measurements.
(24) Kochi, M.; Mita, I.; Horigome, T.; Yokota, R. In *Proceedings of 2nd International Conference on Polyimides*; Society of Plastics Enginners: Ellenville, NY, 1985; p 454. The s-BPDA/ODA films annealed at $T_{ann} \geq 300$ °C show no precrystallization exthothermic peak in the DSC thermograms.
(25) Vladimirov, L. In *Recent Advances in Polyimides 1997* (*Proceedings of Japan Polyimide Conference '96*, Tokyo); Yokota, R., Hasegawa, M., Eds.; Raytech Co.: Tokyo, p 13; will be submitted to *Macromolecules*.
(26) Gerber, M. K.; Pratt, J. R.; St. Clair, T. L. In *Polyimides: Materials, Chemistry, and Characterization*; Feger, C., Khojasteh, M. M., MacGrath, J. M., Eds.; Elsevier: Amsterdam, 1989; p 487.
(27) Tamai, S.; Yamaguchi, A.; Ohta, M. *Polymer* **1996**, *37*, 3683.
(28) Our semiempirical MO calculation (AM1 and PM3) for biphenyl ether suggests that there is no significant barrier for the conformational change.
(29) Unpublished results; the T_g of s-BPDA/PDA cured at 200 °C for 3 h + 400 °C for 1 h, which is indistinct (see Figure 7b), was estimated from the extrapolation for the T_g's of s-BPDA: a-BPDA/PDA copolymers (s-BPDA = 0−90 mol %) cured under the same conditions.
(30) Mita, I.; Yokota, R.; Kambe, H. *Rep. Prog. Polym. Phys. Jpn.* **1971**, *16*, 319.
(31) Dine-Hart, R. A.; Wright, W. W. *Makromol. Chem.* **1971**, *143*, 189.
(32) Ando, S.; Kuroko, H.; Ando, I. In *Recent Advances in Polyimides 1996* (*Proceedings of Japan Polyimide Conference '95*, Tokyo); Imai, Y., Kakimoto, M., Eds.; Raytech Co.: Tokyo, 1996; p 92.
(33) Kowalczyk, S. P.; Stafström, S.; Bredas, J. L.; Salanek, W. R.; Jordan-Sweet, J. L. *Phys. Rev.* **1990**, *41*, 1645.
(34) *Ultra-violet and Visible Spectroscopy: Chemical Applications*, 2nd ed.; Rao, C. N. R., Ed.; Butterworth: London, 1967; pp 154−162.
(35) Suzuki, H. *Bull. Chem. Soc. Jpn.* **1959**, *32*, 1340, 1350, 1357.
(36) Hasegawa, M.; Shindo, Y.; Sugimura, T.; Ohshima, S.; Horie, K.; Kochi, M.; Yokota, R.; Mita, I. *J. Polym. Sci., Part B* **1993**, *31*, 1617.

MA9808629